Future prospects for the measurement of direct photons at the LHC

David Joffe[1] on behalf of the ATLAS and CMS Collaborations

[1]Southern Methodist University Department of Physics, 75275 Dallas, Texas, USA

The energy scale of the LHC, as well as the large size of the ATLAS and CMS experiments, present new challenges for the detection of direct photons as well as new opportunities for physics observations. This talk will examine the direct photon energy and momentum measurement capabilities of the two general purpose experiments for both converted and unconverted photons, and the resulting prospects for diphoton physics channels such as H$\rightarrow \gamma\gamma$.

The Large Hadron Collider at CERN will provide an exciting new window into the physics of high-energy direct photons. For the LHC running at design energy, direct photon production (for photons with $p_{\mathrm{T}} \geq 20$ GeV) is expected to have a cross-section of 100 nb, and for photon pairs (both with $p_{\mathrm{T}} \geq 20$ GeV) the expected cross-section is 15 nb. The diphoton channel is also considered to be key for the discovery of a low-mass (120-140 GeV) Standard Model Higgs boson, but the relatively low diphoton branching ratio ($\sim 10^{-3}$) means that the effective cross-section for H$\rightarrow \gamma\gamma$ at the LHC is of the order of 20 fb, 6 orders of magnitude below the non-resonant direct diphoton cross-section. The ability to observe such a rare decay requires a very good understanding of the detectors. The relatively narrow (MeV-scale) decay width of the Standard Model Higgs boson in the low-mass range means that the measured width of any Higgs boson signal will be dominated by the detector resolution; such a signal should be visible as a small enhancement of the diphoton mass spectrum, requiring a detector resolution of order $\sigma(\mathrm{m})/\mathrm{m} \sim 1\%$, as well as a high level of rejection of jets and neutral pions. This note will attempt to summarize the energy and momentum measurement capabilities of the two general purpose experiments, and their ability to observe H$\rightarrow \gamma\gamma$ and other rare TeV-scale diphoton decays such as those predicted in universal extra-dimension theories [1].

1 The ATLAS and CMS detectors at the LHC

The ATLAS and CMS detectors are located at the Large Hadron Collider (LHC) at CERN. For proton-proton collisions, the LHC is designed to run with $\sqrt{s}$=14 TeV, with a bunch crossing frequency of 25 ns. The design luminosity for the LHC is 10^{33} cm^{-2} s^{-1} for low-luminosity initial operation, and 10^{34} cm^{-2} s^{-1} for high-luminosity operation. These energies and luminosities require a very large size and fine granularity for the detectors. Because of the unprecedented amount of material in the tracking detectors, particular attention has to be paid to material effects, particularly to photon conversions in the context of this paper. Further information

about the construction and expected performance of the general-purpose experiments can be found in refs. [2] and [3] for ATLAS, and refs. [4], [5] and [6] for CMS.

The dimensions of the ATLAS detector are 25 m in height and 44 m in length, with a 2 Tesla solenoidal magnetic field in the inner volume, and an overall mass of the detector of approximately 7000 tonnes. The CMS detector is more compact, but also more massive; it measures 15 m in height and 21 m in length, with a 4 Tesla solenoidal magnetic field and an overall mass of $\sim$12500 tonnes. The most crucial components of the detectors for direct photon measurements are the electromagnetic (EM) calorimeters; ATLAS and CMS use very different techniques in their calorimetry. The ATLAS EM calorimeter is a Liquid Argon (LAr) sampling calorimeter with three sampling layers with the middle sampling layer consisting of 86,400 channels. The CMS EM calorimeter is composed of $\sim$80,000 lead tungstate ($PbWO_4$) scintillating crystals. These two very different calorimeters each have their own strengths; the ATLAS LAr calorimeter, with its multiple sampling layers, is able to reconstruct shower shapes in all three dimensions, thereby providing excellent electron and photon identification, while the CMS EM calorimeter has extremely accurate energy reconstruction.

Both the ATLAS and the CMS EM calorimeters are highly segmented. The front layer of the ATLAS calorimeter is comprised of narrow strips with widths of 0.003 in η, and middle and back layers with widths of 0.025 in ϕ. The CMS EM calorimeter has a granularity of $\Delta\eta \times \Delta\phi = 0.0175 \times 0.0175$ in the barrel region. This fine segmentation is crucial for accurate reconstruction of narrow diphoton resonances.

Both the ATLAS and CMS detectors contain multi-layered inner trackers which direct photons must cross before reaching the calorimeters. The material in these inner trackers is substantial; in the case of ATLAS, there is approximately 0.5 radiation lengths of inner-detector material in the central region, and as much as 2 radiation lengths in the region around $|\eta| = 1.7$, and for CMS the numbers range from 0.4 radiation lengths in the central region to as much as 1.5 radiation lengths around $|\eta| = 1.7$. As the probability for photons to convert to e^+e^- pairs is proportional to the number of radiation lengths traversed, this large amount of material means that direct photons have a probability of $\sim 20\%$ of converting in the central region, and up to a maximum probability of $\sim 60\%$ of converting at larger $|\eta|$. Figure 1 shows probabilities of conversion for photons in the ATLAS detector as well as the positions of photons converted in the ATLAS inner detector as simulated in GEANT4 [3]; the tracking layers are clearly visible.

Efficiently reconstructing and identifying photon conversions while preserving the best possible EM calorimeter resolution is a challenging task. Figure 2 shows the efficiency of reconstruction of photon conversions in the ATLAS detector as a function of conversion radius and η, for photons from H$\rightarrow \gamma\gamma$ decay. In this figure, the points with error bars show the total reconstruction efficiency, the solid histograms show the conversion vertex reconstruction efficiency, and the dashed histograms show the single-track conversion reconstruction efficiency. Using both tracks with silicon hits, as well as tracks from the Transition Radiation Tracker (TRT), the total reconstruction efficiency ranges from $\sim 90\%$ for photons converting within 15 cm of the beam axis, to $\sim 60\%$ for conversions occuring more than 70 cm from the beam axis; these efficiencies are mostly independent of $|\eta|$ over the geometrical acceptance of the TRT which extends only to $|\eta| \sim 2$.

Both ATLAS and CMS have extremely good energy resolution in their EM calorimeters. For direct photons with energies of 100 GeV, the ATLAS LAr calorimeter has a resolution of better than 1.4% at $|\eta| = 1.075$ [3], while the CMS EM calorimeter has a resolution of better than 0.7% for 120 GeV electrons, after corrections [4]. Figure 3 shows the energy resolution for photons in the ATLAS detector as a function of energy and η; Figure 4 shows the energy resolution

of the ATLAS detector for 100 GeV photons (normalised to the true energy) and the energy resolution for unconverted barrel photon showers in CMS with $R9 \geq 0.943$, reconstructed in a 5×5 crystal array, as a function of energy, together with the fitted parametrization. The equation for the energy resolution in the barrel of the ATLAS LAr calorimeter can be expressed as $\sigma_E/E \approx 10\%/\sqrt{E} + 0.7\%$ [3], while for CMS the relation is given as $(\sigma/E)^2 = (3.6\%/\sqrt{E})^2 + (185(\text{MeV})/E)^2 + (0.66\%)^2$ [4]. The different equations for the relative resolutions reflect the very different properties of the two calorimeters.

To first order, the angular resolution for direct photons is determined by the granularity of the calorimeters; Figure 5 shows the angular resolution for photons in the ATLAS detector; the polar angle resolution from calorimeter layers 1 and 2 for 100 GeV photons is $\sigma_\theta \sim 50$ mrad$/\sqrt{E}$. The angular resolution in ATLAS is improved for the case of converted photons due to the high segmentation of the tracker, particularly in polar angle. For converted photons, the polar angle can be determined to a resolution of 0.3 mrad for photons originating from H$\rightarrow \gamma\gamma$ decays with $m_H = 120$ GeV [3].

Due to the large hadronic backgrounds present at the LHC, rejections of the order of 10^3 or better are required to separate direct photons from jets and neutral pions; this rejection is done primarily through the shower shapes. If isolation cuts are included, rejection rates of up to 10^4 may be achieved [3].

Photons may be reconstructed with quite high efficiencies in the LHC detectors; for photons from H$\rightarrow \gamma\gamma$ with $p_\text{T} \geq 50$ GeV simulated in the ATLAS detector, the efficiency ranges from 80-90% depending on the selection cuts. This efficiency is largely independent of $|\eta|$, with the exception of the region between the barrel and end-cap of the LAr calorimeter around $|\eta| = 1.5$, where it is somewhat reduced [3]. These high efficiencies can be extended up to the TeV energy range; Figure 6 shows the photon reconstruction efficiency for high-p_T photons from the decay of gravitons with a mass of 500 GeV in the ATLAS detector [3].

2 Physics with diphoton resonances

The decay of the Standard Model Higgs boson into two photons is considered a key discovery channel and has been extensively studied in simulation by both ATLAS and CMS. Given the narrow Higgs boson width expected in the low-mass range (115-150 GeV), the shape of the signal is dominated by the energy and angular resolution of the detectors; the observed width of a Higgs boson with a mass of 120 GeV in the ATLAS detector is $\sim$1.4 GeV, with half of the signal events having at least one converted photon.

Due to the large number of diphoton events coming from QCD direct photon production, as well as the misidentification of jets and neutral pions as photons, the Standard Model Higgs boson signal will be observable only on top of a large background; this background is on the order of $\sim$100 times larger than the signal for the inclusive analyses. Thus, sizable statistics will be required to observe any Higgs boson signal with significances of 3σ or more. For the ATLAS standard cut-based combined analysis [3], 10 fb^{-1} of integrated luminosity allows for an observed signal significance of between 3σ and 4σ, depending on the Higgs boson mass. For the CMS optimized analysis [5], a 5σ signal may be observed with between 7 fb^{-1} and 15 fb^{-1} of data, depending on the Higgs boson mass.

The significance vs. luminosity plot for the H$\rightarrow \gamma\gamma$ signal in ATLAS, as well as an invariant mass plot of the signal, are shown in Fig. 7. In the significance plot the solid circles correspond to the sensitivity of the inclusive analysis using event counting. The solid triangles linked

with solid and dashed lines correspond to the sensitivity of the inclusive analysis by means of one dimensional fits, with a fixed and floating Higgs boson mass, respectively. The solid squares linked with solid and dashed lines correspond to the maximum sensitivity that can be attained with a combined analysis. The CMS invariant mass plots for various diphoton channels, including the H→ $\gamma\gamma$ channel, can be seen in Fig. 8, showing the results of a categorized kinematic neural net analysis on the left for all barrel events with a neural net output greater than 0.85, and the cut-based analysis on the right. The neural net analysis is normalised to an integrated luminosity of 7.7 fb^{-1}, and the cut-based analysis to 1 fb^{-1}; the Higgs boson signal in all CMS plots is scaled upwards by a factor 10 for visibility.

As an example of the decay of a high-mass exotic resonance into two photons, both ATLAS and CMS have studied the possibility of observing the diphoton decay of the TeV-scale graviton [1]. Plots showing the significance of discovery for various integrated luminosities in both the H→ $\gamma\gamma$ channel and the G→ $\gamma\gamma$ channel for CMS can be seen in Fig. 9; the left part of the G→ $\gamma\gamma$ discovery limit curve is the region where the significance exceeds 5σ. The limit is shown as a function of the coupling parameter c and the graviton mass for integrated luminosities of 10, 30 and 60 fb^{-1}; the signal is generally observable for graviton masses up to 2 TeV, and may be observable for masses as high as 4 TeV depending on the strength of the coupling parameter.

References

[1] L. Randall and R. Sundrum, Phys. Rev. Lett. **83**, 3370 (1999).

[2] ATLAS Collaboration (G. Aad *et al.*), JINST **3**:S08003 (2008).

[3] ATLAS Collaboration, Expected Performance of the ATLAS Experiment, Detector, Trigger and Physics, CERN-OPEN-2008-020, Geneva (2008).

[4] CMS Collaboration, CMS Physics TDR: Volume I, Detector Performance and Software, CERN-LHCC-2006-001, Geneva (2006).

[5] CMS Collaboration, CMS Physics TDR: Volume II, Physics Performance, CERN-LHCC-2006-021, Geneva (2006).

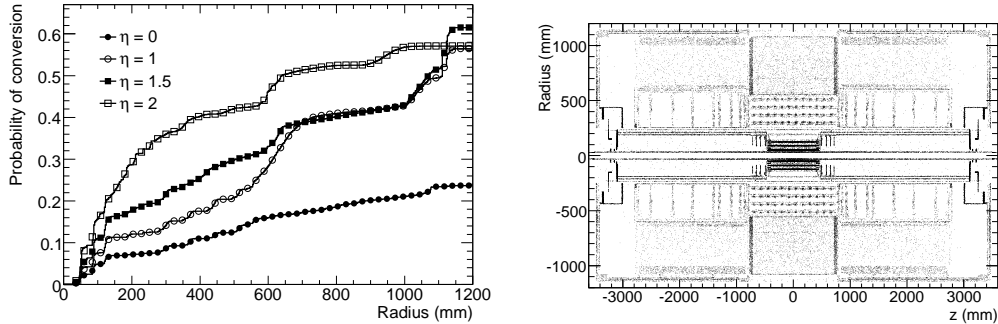[6] CMS Collaboration (S Chatrchyan *et al.*), JINST **3**:S08004 (2008).

Figure 1: Probability of a high-energy photon to convert as a function of radius for different values of η in the ATLAS inner detector (left) and graphical representation of the ATLAS inner detector material in the (z-R) plane as obtained from the true positions of simulated photon conversions in minimum-bias events (right) [3].
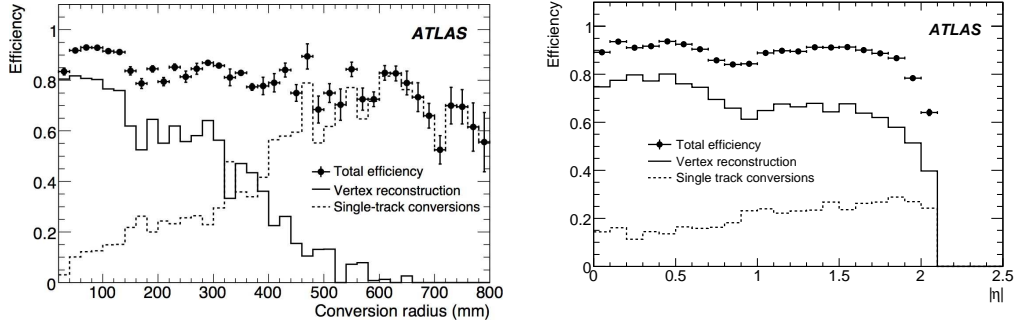
Figure 2: Reconstruction efficiencies for converted photons from H→ γγ decays in the ATLAS detector as a function of conversion radius (left) and pseudorapidity (right) [3].
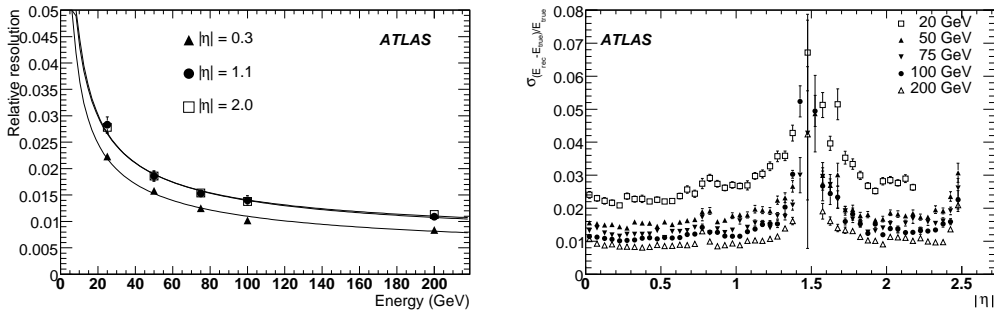

Figure 3: Energy resolution for all photons in ATLAS (left) and energy resolutions for photons in ATLAS (5×5 clusters) (right). [3]
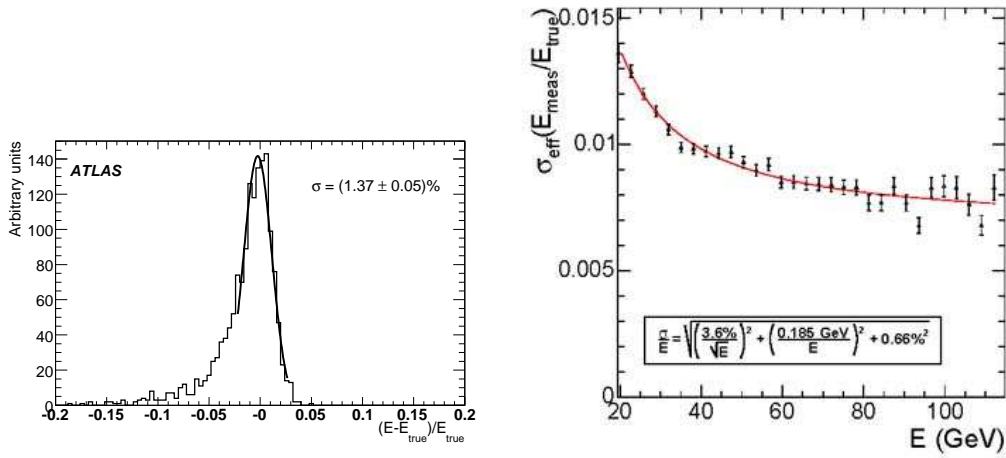

Figure 4: Difference between measured and true energy at E = 100 GeV for ATLAS photons with $|\eta| = 1.075$ (left) [3] and CMS barrel photon energy resolution (right) [4].
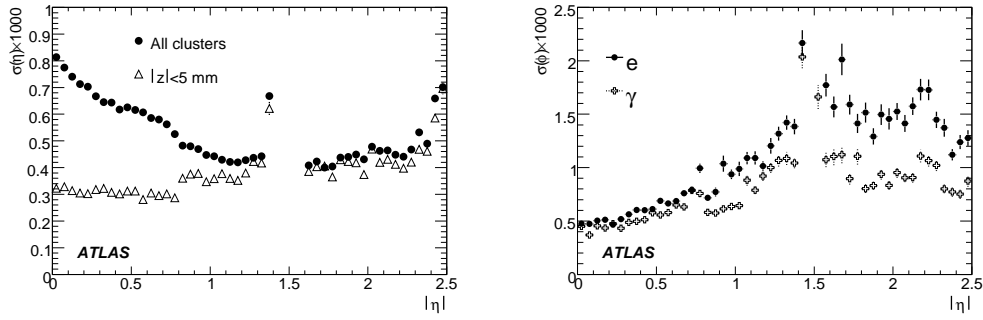
Figure 5: Resolution of η position measurement in ATLAS from calorimeter layers 1 and 2 combined for 100 GeV photons (left) and expected ϕ position resolution in ATLAS as a function of $|\eta|$ for electrons and photons with an energy of 100 GeV. [3]
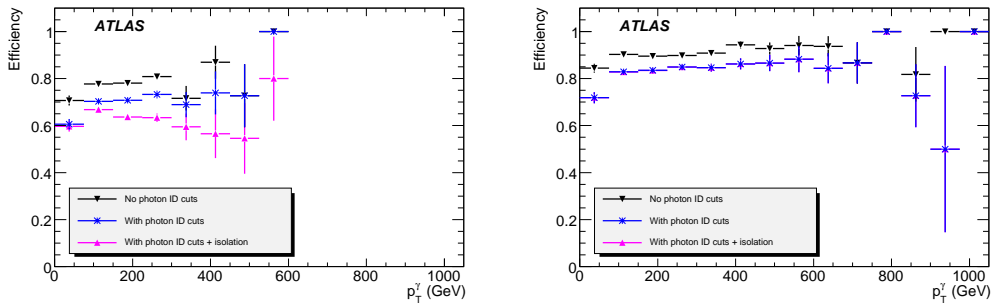

Figure 6: ATLAS photon reconstruction efficiency in the 500 GeV graviton sample as a function of p_T for end-cap (left) and barrel (right) calorimeters. [3]
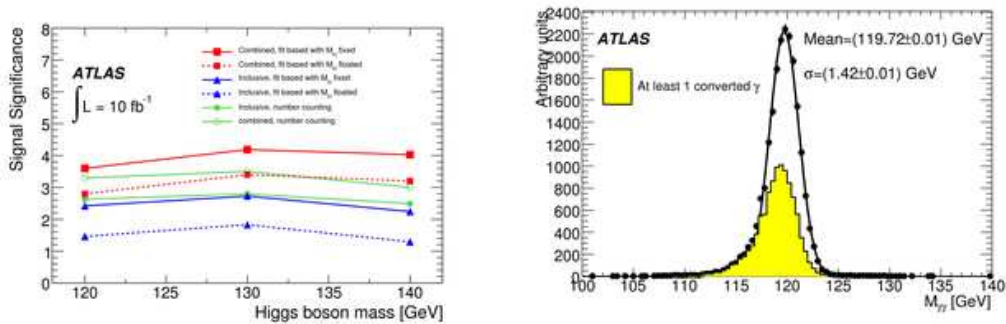

Figure 7: Expected signal significance for a Higgs boson in ATLAS using the H$\to \gamma\gamma$ decay for 10 fb^{-1} of integrated luminosity as a function of the mass (left) and ATLAS diphoton invariant mass distribution after trigger and identification cuts (right); the shaded histogram corresponds to events with at least one converted photon [3].
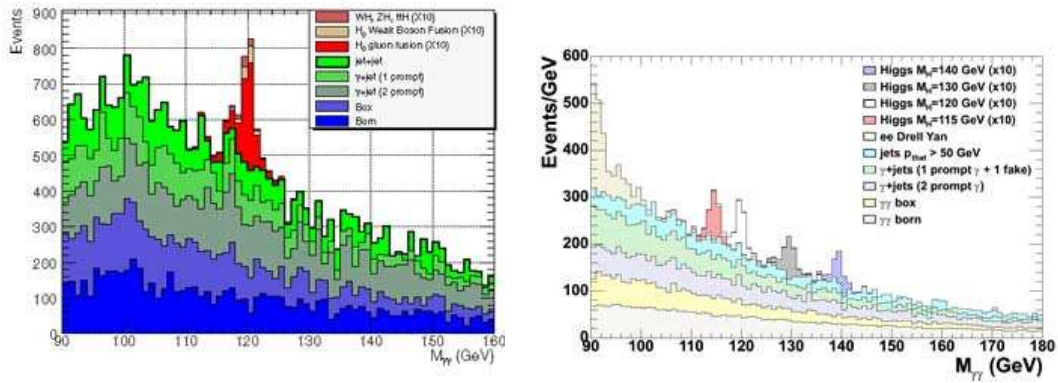
Figure 8: CMS diphoton mass distribution for H→ γγ signal and background after the application of a kinematic neural-net analysis (left), and a cut-based analysis (right) [5].

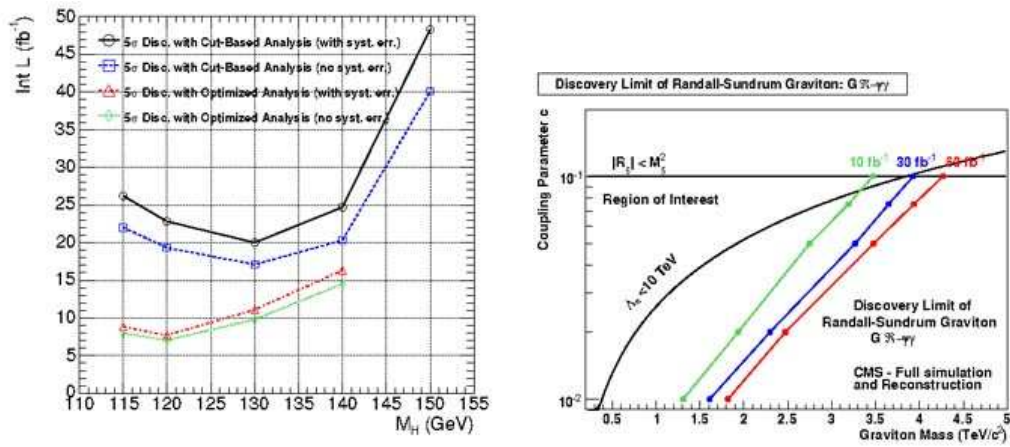Figure 9: Integrated luminosity needed for a 5σ discovery in CMS for the H→ γγ channel (left) and the reach of the CMS experiment in the search for a heavy graviton decaying into the diphoton channel (right) [5].